
GENERAL EXPERIMENTAL TECHNIQUES

An X-ray Refractometer

A. G. Touryanskii and I. V. Pirshin

Lebedev Institute of Physics, Russian Academy of Sciences, Leninskii pr. 53, Moscow, 117924 Russia

Received August 18, 2000

Abstract—A new X-ray refractometer arrangement for investigating the angular and spectral characteristics of refracted radiation in the hard X-ray range is proposed. The refractometer includes two goniometers set along the path of the direct X-ray beam, two crystal analyzers, and three radiation detectors. The maximum distance between the radiation focus and the entrance slit of the second goniometer is 1.4 m. The refractograms of thin-film samples, including a strained C/Si structure, and the dispersion spectrum of an X-ray tube with a copper anode are first measured. A new refractometry technique using sample rocking at a fixed position of the detector device is described. The results of measurements of the refraction rocking curves for fused silica samples and a ZnSe single crystal are presented.

In the first X-ray refraction experiments in [1, 2], the refracting prism was irradiated by a polychromatic X-ray beam. In this case, the refractive index n was determined from the angular positions of the characteristic line peaks in the refracted beam. The intensity distribution behind the prism was recorded on a film, and the direct beam was taken as an angular reference. Angular measurements under such conditions are unambiguous, because the spectral density of the characteristic radiation of X-ray tubes at $\lambda \sim 0.1$ nm exceeds this parameter for the bremsstrahlung spectrum component by more than three orders of magnitude. However, the same cause made it impossible to study the refraction of the bremsstrahlung portion of the spectrum.

Davis and Slack first proposed a two-crystal scheme for measuring the angles of refraction [3, 4]. The sample under study was set in a monochromatic beam between the first and second crystals, and the angle of refraction was determined by the difference of the angular positions of the diffraction peaks before and after sample placement into the beam. Up to recently, no basic changes in the refractometric schemes [1–4] were reported. In [5], we have shown that the angular parameters and intensity of the refracted radiation can be measured by using a two-wave reflectometer [6, 7]. In this case, a sample is irradiated with a polychromatic spectrum, from which two characteristic lines were simultaneously selected by using a beamsplitter based on semitransparent monochromators. Thus, the characteristics of the refracted radiation were measured either in a polychromatic spectrum or in one–two spectral lines in all known refractometric schemes.

This work proposes a new measurement scheme allowing us to extend the functional capabilities of the refractometer and to implement both measurement versions without additional readjustment and alignment of the X-ray optical system.

Figure 1 shows the X-ray optical arrangement of the refractometer in its measurement plane. The radiation source is a sharply focusing X-ray tube 1 with a copper anode (the visible size of the tube focus in the measurement plane is 40 μm ; in the perpendicular direction, the focal size is 8 mm). Two X-ray goniometers are set up on the X-ray beam path. The distances from the focus of the X-ray tube to the principal axes O_1 and O_2 of the goniometers 5 and 17 are 330 and 1161 mm, respectively, and, from the O_1 - and O_2 -axes to the entrance slits 10 and 15, the distances are 225 and 192 mm, respectively. The distances between O_1 and O_2 can be varied by moving the goniometer 17 along the guides in a range of 1050–1250 mm. A beamsplitter with two semitransparent pyrolytic-graphite monochromators 8 and 9 is set up on a rotating bracket of the first (along the beam propagation direction) goniometer 5 behind the entrance slit 10. The characteristic CuK_α and CuK_β lines selected by the monochromators from the analyzed beam are recorded by detectors 12 and 14. Thus, data in the two spectrum regions can be obtained in a single angular-scanning cycle. A detector 16 positioned on a rotating bracket of the goniometer 17 ensures a detection efficiency of $\geq 90\%$ in an energy band of 30 keV and is used to detect polychromatic spectra. For this purpose, the rotating bracket of the goniometer 5 is withdrawn from the direct beam axis. In order to detect weak signals in the soft spectrum region, an evacuated collimator 18 with Mylar end windows is mounted between the sample and entrance slit 15. The technical parameters of the goniometers are identical; therefore, it is possible to bring the beamsplitter 19 and sample holder to the second goniometer.

When a 30- μm -wide entrance slit is used, the system ensures the detection of a refracted radiation with angular resolutions of 0.0076° and 0.0017° at the first and second goniometers, respectively. The typical angular divergence of a probe beam incident on the refracting face of the sample is 0.0055° and 0.0069° .

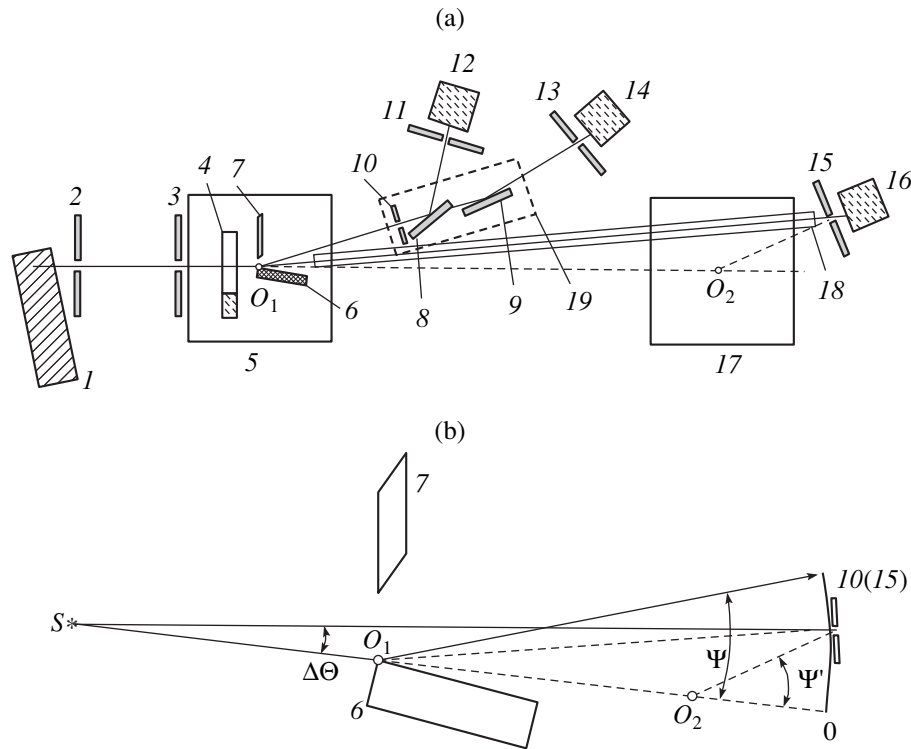


Fig. 1. (a) Layout of the X-ray refractometer: (1) X-ray tube; (2, 3) collimation slits; (4) movable horizontal slit; (5, 17) goniometers; (6) sample; (7) absorbing shield; (8, 9) semitransparent monochromators; (10, 11, 13, 15) entrance slits; (12, 14, 16) radiation detectors; (18) evacuated collimator; and (19) housing of the beamsplitter. (b) Radiation path geometry for beam refraction at the front edge of the sample.

As was shown in [5, 8], refractometric measurements can be performed by using a geometry ensuring successive transmission of an X-ray beam through a lateral shearing cut and an optically polished sample surface or in the opposite succession. In this case, conducting correct angular measurements requires that the principal rotation axis of the goniometer 5 be matched with either the front (along the X-ray beam direction) or back edge of the polished sample surface: this excludes displacement of the refracting edge in the course of sample rotation. In some cases, as is shown below, when working with small samples, the coincidence of the principal axis with the sample's center is expedient. These positions of the sample relative to the principal axis are denoted as *F* (front), *B* (back), and *C* (center). The current angles of rotation ω are measured counterclockwise in the plane of incidence of the probe beam coinciding with the measurement plane. For $\omega = 0$, the ray emerging from the center of the focal spot is tangent to the refracting surface. In accordance with the notations adopted earlier, fixed grazing angles of the X-ray beam with respect to the interface are designated as θ_1 and measured in the positive direction independently of the sample orientation.

For a sample set up in the *F* or *B* position and subsequent angular scanning of the entrance slit 10 together with elements 11–14, the angles of deviation

Ψ between the primary and refracted beam directions can be directly measured (Fig. 1b). For this purpose, the point of intersection between the line running through the focal spot center and the sample rib with the circle of the slit 10 rotation should be chosen as the zero angular direction of the receiving device.

If the second goniometer is used, it is necessary to translate the angles of rotation Ψ' of the entrance slit 15 about the O_2 -axis into the angles of deviation Ψ measured upon rotation about the O_1 -axis. From the geometry of the rays shown in Fig. 1, we obtain

$$\Psi = \arctan [R_2 \sin \Psi' / (L_0 + R_2 \cos \Psi')], \quad (1)$$

where R_2 is the distance from O_2 to the entrance slit 15, and L_0 is the distance between the principal axes O_1 and O_2 of the goniometers 5 and 17. For $\lambda \sim 0.1$ nm, typical values of the measured angles satisfy the condition $\Psi < \Psi' < 1^\circ$. Expanding (1) into a series in terms of Ψ' near the point $\Psi' = 0$ yields

$$\Psi \approx R_2 \Psi' / (L_0 + R_2). \quad (2)$$

Let us estimate the effect of the deviation of the entrance slit 15 from the plane normal to the radius vector which connects the point of intersection of the O_1 -axis with the measurement plane and the center of the slit 15. For simplicity, we assume that the beam incident onto the slit is parallel, and the material of the slit has

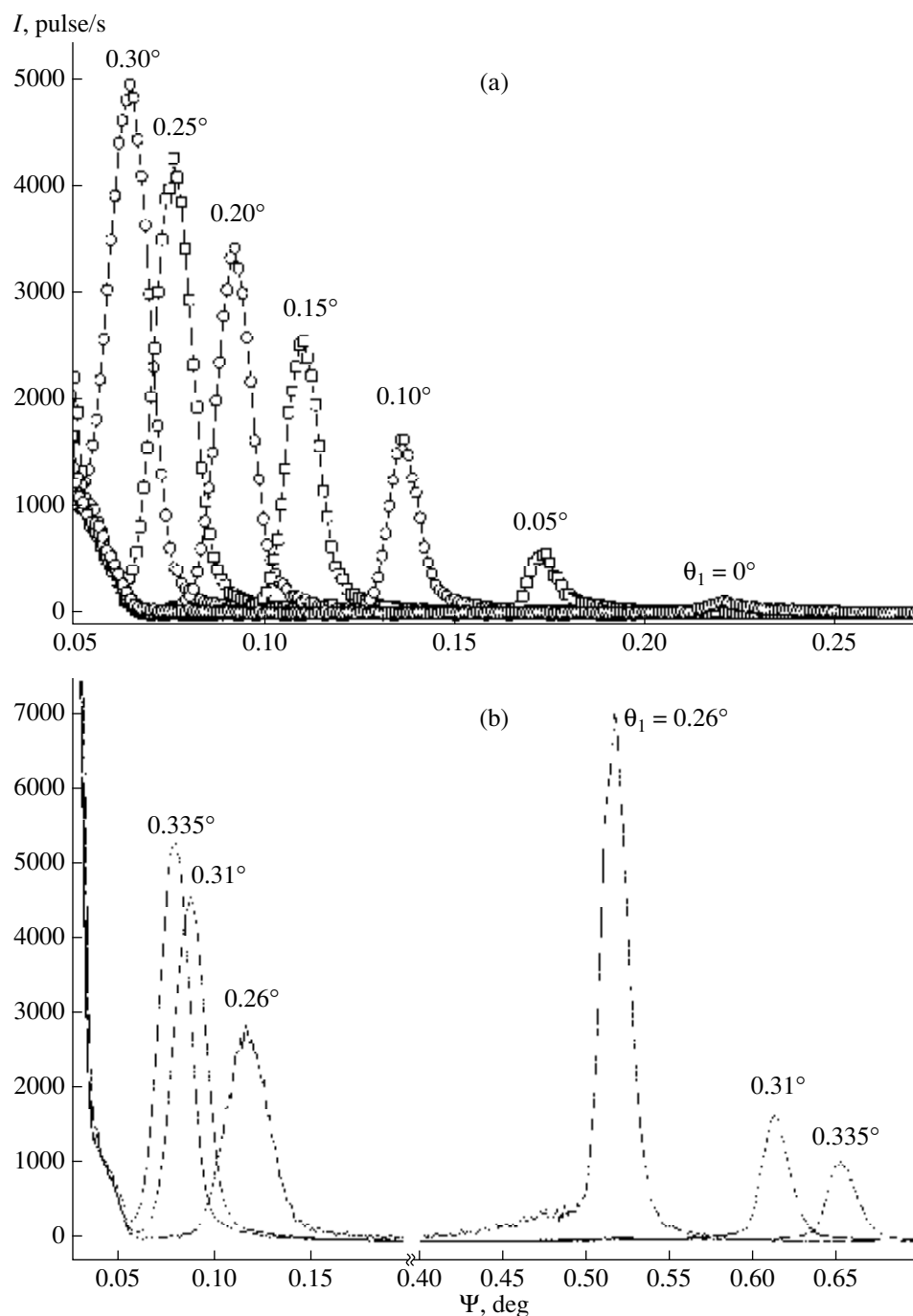


Fig. 2. A series of refractograms for fused silica (SiO₂) at the CuK_α-line for various grazing angles θ_1 of the primary beam in the (a) *F* geometry (incidence from inside) and (b) *B* geometry (incidence from outside).

100% absorption. In practice, the slit is usually formed by blades shaped as wedges with angles of 84°–85°, so that the angle between their faces forming the slit gap is 8°–10°. Since the maximum angle of rotation of the detector *16* about the O_2 -axis is usually $\leq 3^\circ$, the effective gap width of the slit *15* rotated by an angle Ψ' is

$$h_e = h \cos(\Psi' - \Psi), \quad (3)$$

where h is the distance between the slit blades, and Ψ recalculated by using formula (1) is the angle of deviation.

Substituting the maximum (0.5°) and typical (0.2°) values at $\Psi \lambda \sim 0.1$ nm into (2) and (3), we obtain relative changes h_e equal to 0.1 and 0.01%, respectively, which are significantly smaller than a typical statistical counting error ($\geq 1\%$) in the detection of the refracted radiation; therefore, in practice, they can be neglected.

When pyrographite monochromators are used, the angular resolution of the goniometer *5* is determined by the size of the entrance slit *10*. It can obviously be

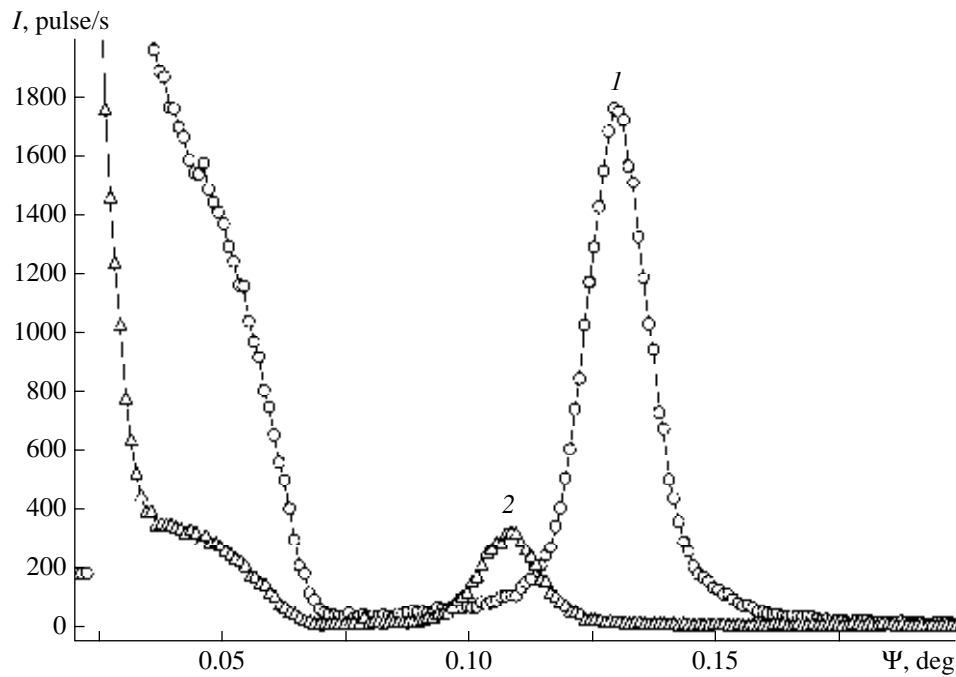


Fig. 3. Angular profiles of the refracted beams for a polished ZnSe single-crystal plate measured in the F geometry at the $\text{CuK}\alpha$ -line (curve 1) and $\text{CuK}\beta$ -line (curve 2) for $\theta_1 = 0.31^\circ$.

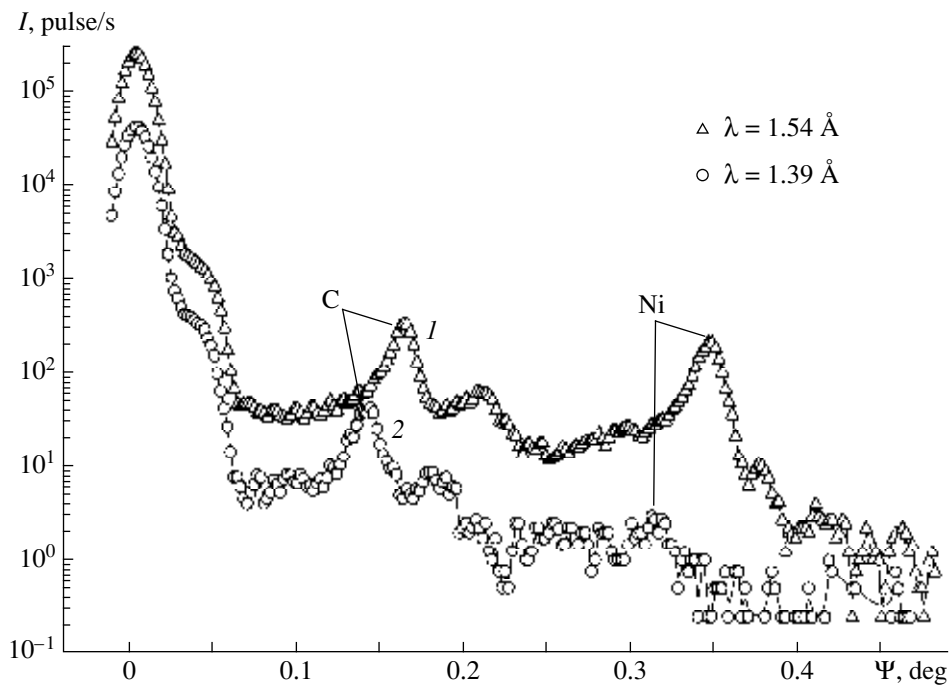


Fig. 4. A refractogram for a C/Ni (36/110 nm) bilayer on a Si substrate for $\theta_1 = 0.053^\circ$: (1) $\text{CuK}\alpha$ and (2) $\text{CuK}\beta$.

increased to a significant degree by replacing pyrographite with a perfect crystal, such as Si or Ge. In this case, the design of a grid type monochromator proposed by us [9] retains the possibility of detecting simultaneously two spectral lines; however, this leads to a decrease in the radiation efficiency of the device

and complication of the adjustment unit located on the rotating bracket of the goniometer. Therefore, such a replacement is reasonable only when studying spectra with fine structures under conditions that the diffraction-induced broadening of the refracted beam can be neglected.

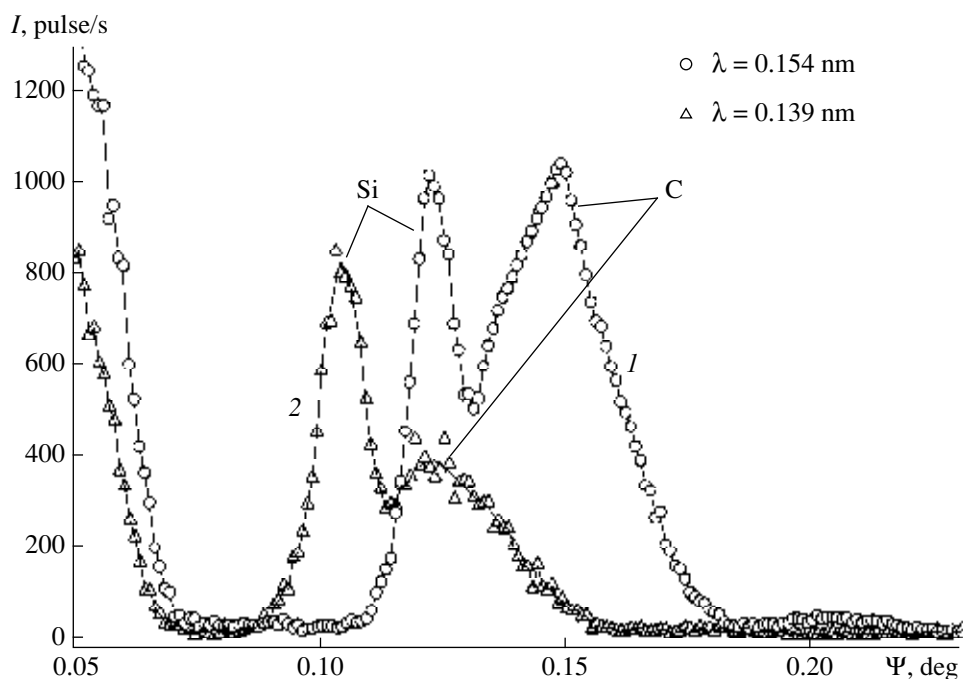


Fig. 5. A refractogram for a strained structure of a diamond-like C film (56 nm) on a Si substrate for $\theta_1 = 0.14^\circ$: (1) $\text{CuK}\alpha$ and (2) $\text{CuK}\beta$.

RESULTS OF TEST MEASUREMENTS

The initial procedure of refractometric measurements is the determination of the zero and detecting unit positions. If the gap between the absorbing screen 7 and sample 6 is small as compared with the effective width of the beam's normal cross section, then the intensity distribution over the gap cross section can be considered uniform. The center of gravity of the direct beam traveling through the gap with a width d is then shifted relative to the beam incident on the sample rib by the quantity

$$\Delta\Theta = d(L_1 + R_1)/(2L_1R_1), \quad (4)$$

where L_1 is the distance between the tube focus and the O_1 -axis, and R_1 is the distance from the O_1 -axis to the entrance slit 10.

The value of d can be measured from the angle of the full overlap of the direct beam and the sample with a known size of the reflecting surface. The other parameters involved in (4) are usually known with an error of ≤ 1 mm. For example, if the gap width is equal to the visible focus size ($\approx 40 \mu\text{m}$), then, for the aforementioned geometrical parameters of the system, $\Delta\Theta = 0.0086^\circ$.

Figure 2 shows two series of the refractograms of an optically polished fused silica plate (SiO_2) at the $\text{CuK}\alpha$ -line measured for direct beam incidence onto the refracting face from inside (the F geometry) and outside (the B geometry). These data were obtained by scanning the rotating support of the goniometer 5 with the slit 10 at several fixed grazing angles θ_1 of the probe beam rela-

tive to the refracting surface. The angular positions of the refraction peaks change strictly according to the law of sines. The total intensity under the peak of the refracted beam is due to the imaginary part of the decrement of n . This allows us to unambiguously determine the X-ray optical constants of the material in the surface layer of the sample [5].

In the right part of Fig. 2b, specular-reflection peaks are shown: their maxima in the angular diagram must be at an angle $\Psi = 2\theta_1$ in the C geometry. In the B geometry, the equality is valid only for the sample with a visible size at an angle θ_1 much smaller than the direct-beam cross section. Specular-reflection peaks are not usually observed in the F geometry, because the reflected beam is directed into the sample bulk and, as a rule, is fully absorbed by its substance.

Figure 3 shows the angular profiles of the reflected beams for a polished ZnSe single-crystal plate in the F geometry obtained at the $\text{CuK}\alpha$ (curve 1) and $\text{CuK}\beta$ (curve 2). Allowing for a correction of the angular displacement of the direct beam, the angular positions of the refracted radiation peaks correspond to the calculated positions derived from the law of sines with the use of the tabulated values of the refractive index decrement [10] and density [11]. Hence, the X-ray optical parameters of the material can be refined by comparing the data obtained either at different grazing angles, θ_1 , or at different wavelengths and fixed θ_1 .

If there are layers with different n near the sample surface, then a split angular diagram of the refracted radiation can be expected for a chosen spectral line.

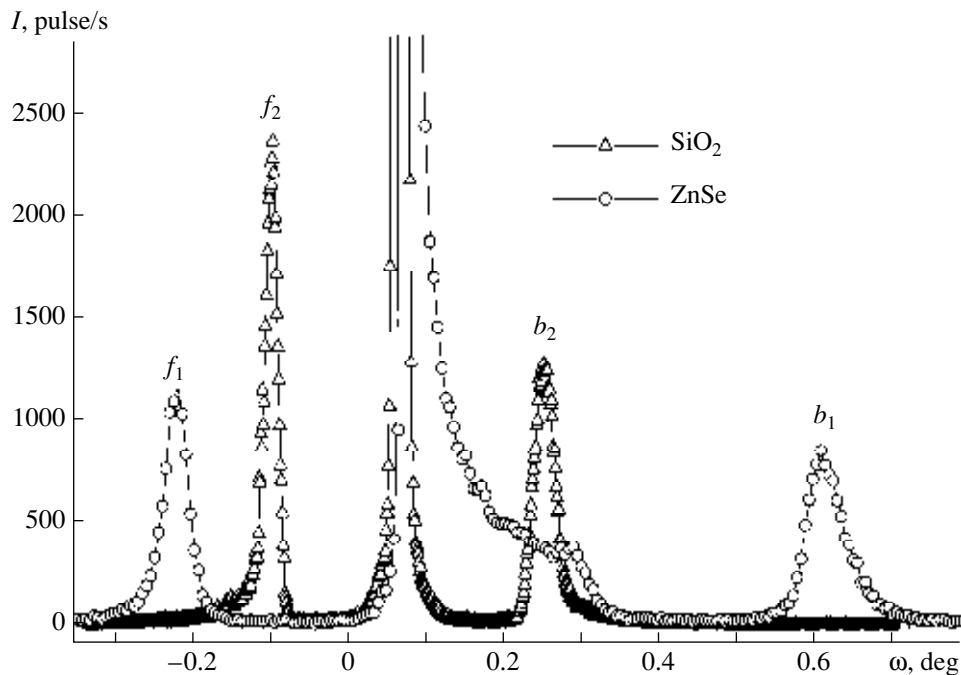


Fig. 6. Refraction rocking curves $I(\omega)$ at a fixed angle of deflection Ψ_0 for ZnSe ($\Psi_0 = 0.16^\circ$) and K8 glass ($\Psi_0 = 0.135^\circ$) samples at the $\text{CuK}\alpha$ -line; f_1, f_2 and b_1, b_2 are the refraction peaks from ZnSe and fused silica, respectively, for the beams passing through the front and rear edges of the samples.

Figure 4 presents refractograms for a Si sample on whose surface Ni (110 nm) and C (36 nm) layers were sequentially deposited by the thermal evaporation technique. The refractogram at the $\text{CuK}\alpha$ line (curve 1) has two pronounced peaks caused by refraction in the C and Ni layers. The magnitude of the Ni peak at the $\text{CuK}\beta$ line (curve 2) is much smaller than that at the $\text{CuK}\alpha$ line. This is determined by the K -jump of photo-absorption resulting in a sixfold increase in the mass attenuation factor for Ni. The refracted radiation from the substrate cannot be observed at a grazing angle $\theta_1 = 0.053^\circ$, because, in the case of incidence from inside, total internal reflection occurs at the Si/Ni interface. The intensity modulation between the refraction peaks and at their wings is due to interference effects in the C film. From the angular positions of the refraction peaks, it follows that the densities of the C and Ni films are 2.2 and 8.9 g/cm^3 , respectively.

A specific feature of refractometric measurements is the comparatively small size of the effective refracting surface in the plane of beam incidence. This size is characterized by the distance l_e over which the amplitude of the wave incident onto the interface is attenuated by a factor e . For example, for a ZnSe sample, $l_e = 54 \mu\text{m}$ at the $\text{CuK}\alpha$ -line. This is two–three orders of magnitude smaller than the typical dimensions of samples used in X-ray reflectometry. Therefore, strained film structures with radii of curvature below 10 m can be suitable for measurements, since a displacement along the surface by the aforementioned l_e value causes

a negligibly small change in the angle between the surface and the incident beam.

Figure 7 shows a refractogram of a single-crystal Si plate 0.35 mm thick, on which a 56-nm-thick C film was grown by the pulsed plasma evaporation technique. Pronounced separation of the peaks from the substrate and film is observed at a grazing angle $\theta_1 = 0.14^\circ$. The film density calculated from the angular position of the refraction peak is 3.05 g/cm^3 . This value indicates that the near order in the C film is characterized by a diamond-like structure.

Assume that, at an arbitrary angular position of a sample in a given range of rocking angles ω , the experimental system ensures the incidence of the direct beam on the opposite edges of the sample surface, as well as the passage of the refracted radiation through the gap between the sample surface and absorbing shield 7 for a specified wavelength from the range in use. Then, at a fixed angular position Ψ_0 of the entrance slit 10, the refracted beam must deviate by an angle Ψ_0 twice per cycle of angular sample scanning: when shifting from the region of negative angles ω to the region of positive ω , the entrance slit first receives the radiation passing through the side face to the refracting surface near its front edge and then the radiation arriving from outside at the other edge of the surface and emerging through the opposite side face. These conditions can obviously be provided for small-sized samples, when the sample's center lies on the O_1 -axis (the \bar{C} geometry).

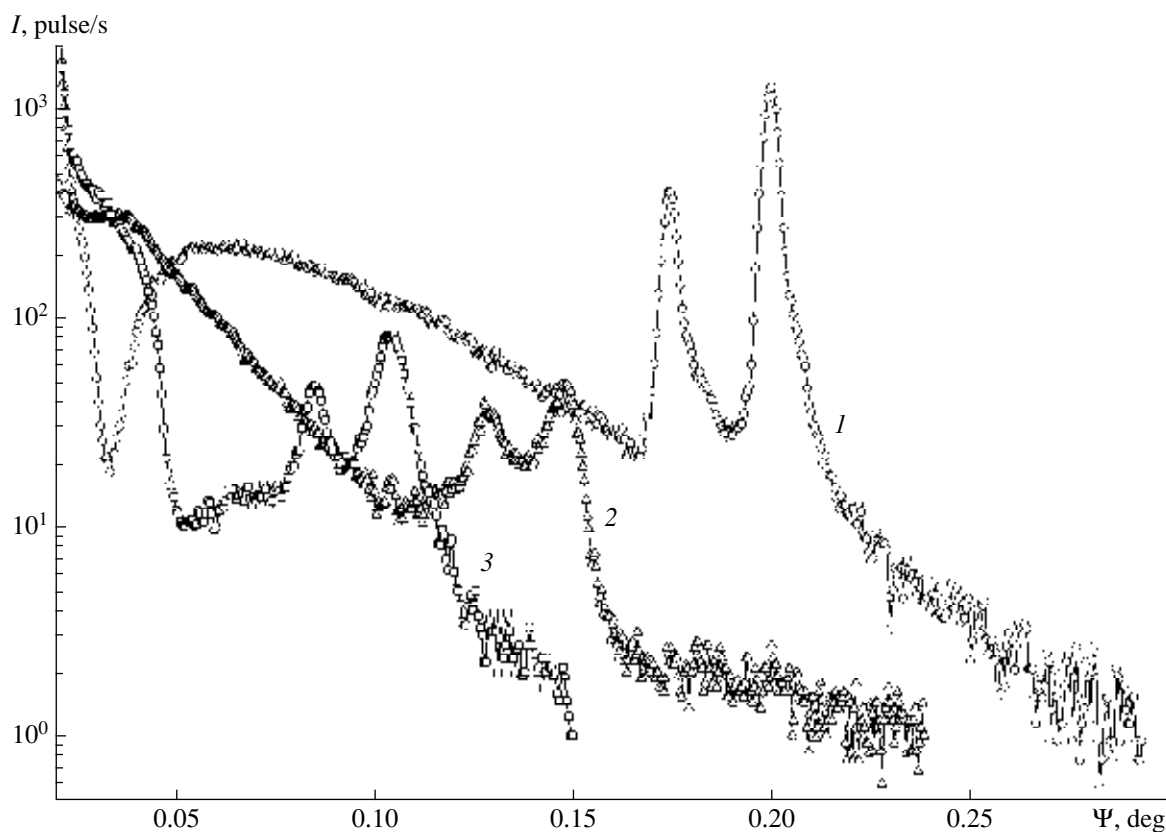


Fig. 7. Refractograms in the polychromatic radiation of a copper-anode tube at $U = 25$ kV: (1) natural diamond ($\theta_1 = 0.08^\circ$); (2) Si single crystal ($\theta_1 = 0.08^\circ$); and (3) GaAs single crystal ($\theta_1 = 0.4^\circ$).

Figure 6 shows refraction rocking curves $I(\omega)$ for ZnSe and fused silica samples confirming the above conclusion. Each of the samples produces two pronounced peaks at negative and positive ω values: f_1 , b_1 for ZnSe and f_2 , b_2 for SiO₂. An intense maximum between the refraction peaks truncated at a level $I(\omega) = 3000$ pulse/s is determined by specular reflection from the sample turned by an angle $\omega = \Psi_0/2$. Allowing for corrections for a finite SiO₂ sample size, the calculated and measured angular distances between the peaks f_2 and b_2 coincide within $\sim 1\%$. The peak of the specular reflection from ZnSe is asymmetric and shifted with respect to the expected angular position by $\sim 0.1^\circ$. This feature can be caused by one of the edges of the reflected surface rounded as a result of a finishing treatment of the ZnSe disk in a polishing etcher. When the plate was subsequently split off along the scribing lines, one of its sides was in the immediate vicinity of the edge of the initial disk. This conclusion is confirmed by an increase in the angular distance between the refraction peaks f_1 and b_1 by 0.21° as compared to the calculated value for a flat ZnSe sample.

Measurements in polychromatic radiation allow us to compare the X-ray spectra before and after the radiation is transmitted through a sample in a wide spectral range. When a standard sample is selected, one can

solve an inverse problem: to reconstruct the spectrum of the initial radiation from the angular intensity distribution. If measurements are performed in air, then, as a result of intense absorption of the soft part of the X-ray spectrum on a path length of ~ 1 m, the long-wavelength limit lies between 0.25 and 0.30 nm. The short-wavelength limit is formally restricted only by the angular resolving power of the refractometer and dispersive characteristics of the sample under study.

Figure 7 shows the refractograms of natural diamond (curve 1) and Si (curve 2) and GaAs (curve 3) single crystals. These data were obtained by angular scanning of the detector *I6* with an entrance slit $30 \mu\text{m}$ wide attached to the rotating support of the second goniometer. The CuK_α and CuK_β lines are resolved in the spectra of the Si and GaAs samples. However, the short-wavelength spectrum limit is not separated from the direct-beam wing. Under similar measurement conditions, the diamond sample ensures a much higher (by more than an order of magnitude) average intensity of the refracted radiation and the possibility of analyzing the spectrum at wavelengths of < 0.05 nm.

The above results show that the scheme described makes it possible to precisely measure the angles of refraction and intensity distributions for monochromatic and polychromatic radiations. A rather wide vari-

ety of optically polished samples regardless of their structure and composition can be investigated in this refractometer. The instrument can be used to solve two main types of problems: (1) to measure the parameters of surface layers and the surface geometry by using the spectral lines, for which the X-ray optical parameters of all chemical elements are reliably known; (2) to measure intense X-ray spectra in a small solid angle with the help of a refracting sample, for which the absorption jumps lie outside of the spectrum region under consideration, and the X-ray optical parameters are tabulated over the entire spectral range.

Determining the parameters of a thin film and, especially, strained structures with a radius of curvature $R < 10$ m, which are produced by heteroepitaxy and other deposition techniques, is of special interest for analytical problems of the first type. The possibility of such measurements was first shown in this study for the example of samples with a C/Ni bilayer and a diamond-like C film on a Si substrate.

Rocking-curve refractometry of a sample allows one to collect additional information not only on the average value of R but also on the R variation along the line of intersection of the tested surface with the measurement plane. The data obtained with this technique for fused silica and ZnSe single-crystal samples are also presented for the first time.

The possibility of solving second-type problems concerned with X-ray spectrometry is confirmed by the results obtained in a polychromatic spectrum by using a sample of natural diamond as a refracting element. It is obvious that, if a one-dimensional position-sensitive detector is mounted on the second goniometer, the spectra of pulsed radiation sources can be measured.

ACKNOWLEDGMENTS

We are grateful to I.P. Kazakov, Yu.V. Korostelin, Yu.P. Pershin, V.M. Roshchin, and R.A. Khmel'nitskii for the samples used in the experiments.

This work was supported by the Russian Foundation for Basic Research, project no. 00-02-16470.

REFERENCES

1. Larsson, A., Siegbahn, M., and Waller, T., *Phys. Rev.*, 1925, vol. 25, p. 235.
2. Larsson, A., Siegbahn, M., and Waller, T., *Naturwissenschaften*, 1924, vol. 12, p. 1212.
3. Davis, B. and Slack, C.M., *Phys. Rev.*, 1925, vol. 25, p. 18.
4. Slack, C.M., *Phys. Rev.*, 1926, vol. 27, p. 691.
5. Touryanskii, A.G. and Pirshin, I.V., *Prib. Tekh. Eksp.*, 1999, no. 6, p. 104.
6. Touryanskii, A.G., Vinogradov, A.V., and Pirshin, I.V., *Prib. Tekh. Eksp.*, 1999, no. 1, p. 105.
7. Touryanskii, A.G., Vinogradov, A.V., and Pirshin, I.V., US Patent 6 041 098, Class 378-70.
8. Touryanskii, A.G., Kazakov, I.V., Pirshin, I.V., and Rzaev, M.M., Abstracts of Papers, *Natsional'naya konferentsiya po primeneniyu rentgenovskogo i sinkhrotron-nogo izlucheniya neitronov i elektronov (RSNE-97)* (Nat. Conf. on Application of X-ray and Synchrotron Radiation of Neutrons and Electrons), Dubna: Joint Inst. for Nucl. Res., 1997, p. 145.
9. Touryanskii, A.G. and Pirshin, I.V., *Prib. Tekh. Eksp.*, 2000, no. 4, p. 117.
10. Henke, B.L., Gullikson, E.M., and Davis, J.C., *At. Data Nucl. Data Tables*, 1993, vol. 54, no. 2, p. 181.
11. *Fizicheskie velichiny. Spravochnik* (Physical Parameters: A Handbook), Grigor'ev, I.S. and Meilikhov, E.Z., Eds., Moscow: Energoatizdat, 1991.